Geophys. J. Int. (2002) **151,** 944–949

RESEARCH NOTE

The hydroelectric problem of porous rocks: thermodynamic approach and introduction of a percolation threshold

André Revil

CNRS-CEREGE, Department of Hydrogeophysics and Porous Media, BP 80, *Cedex* 4, 13545 *Aix-en-Provence, France. E-mail: revil@cerege.fr*

Accepted 2002 June 11. Received 2002 May 16; in original form 2002 January 7

SUMMARY

An electrical field is produced in response to groundwater flow in porous materials such as soils and permeable rocks. This electrical field is due to the relative displacement between the charged mineral grains and the pore water, which drags the excess of electrical charge located in the close vicinity of the pore water/mineral interface in the so-called electrical double layer. In this note, I take the hydroelectric problem back to its thermodynamic roots by showing how the hydroelectric equations can be derived from the Gibbs-Duhem equation. In addition, I suggest that the introduction of a percolation porosity may improve the description of the material properties of granular porous materials entering the coupled hydroelectric problem at the macro-scale. Comparison between the proposed model and a set of laboratory data available from the literature are in agreement for a reasonable choice of specific parameters.

Key words: electrical transport, percolation, permeability, porous medium, streaming potential.

1 INTRODUCTION

The study of the groundwater flow in the subsoil is a very difficult problem due to the very high range covered by the hydraulic properties of porous soils and rocks. For example, permeability of sand clay mixtures varies over 12 orders of magnitudes (e.g. Revil & Cathles 1999). There is clearly a lack of methods available to determine the spatial variations of the key hydraulic parameters or to visualize the pattern of groundwater flow in the subsurface of the Earth. The classical use of piezometers to monitor the water head has several drawbacks including (1) the fact that the hydraulic head is obtained only at discrete locations, (2) the existence of hydraulic perturbations associated with the use of piezometers, and (3) the cost and time associated with the installation of a set of piezometers. There is also a lack of efficient geophysical tools available to measure at distance (without perturbation) the pattern of fluid pressure distribution in the subsoil associated for example with a pumping test in a borehole.

A new method could arise from the study of the electrical field generated by the flow of the groundwater itself. This electrical field is due to the relative displacement between the charged mineral grains and the pore water, which drags the excess of electrical charge located in the close vicinity of the pore water/mineral interface into the so-called electrical double layer (e.g. Revil & Leroy 2001). This phenomenon produces a net current density, which serves as source term in the Maxwell equations. This effect is known as the streaming potential and is one of the so-called electrokinetic effects. In addition this electric field is high enough to be recorded at the ground surface using non-polarisable electrodes (e.g. Revil *et al.* 2002). This 'hydro-electric' conversion represents therefore an appealing signal to geophysicists to study the pattern of groundwater flow in the subsurface of the Earth (Birch 1998; Ishido & Pritchett 1999; Trique *et al.* 1999). The development of new methods to invert the electrical field at the ground surface in order to determine the hydraulic source at depth (that Revil *et al.* in press, termed 'electrography') could represent a breakthrough in this direction.

In this paper, I first discuss the thermodynamic roots of the electrokinetic coupling in the context of 'generalized' linear thermodynamics. I then discuss the origin of the equality between the two coupling terms arising into the hydroelectric problem. In Sections 3 to 6, I show that the introduction of a percolation threshold in the transport properties (electrical conductivity, permeability, and electrokinetic coupling coefficient) improves the predictive capabilities of the equations developed on the basis of a differential effective medium model, which, by construction, does not possess such a percolation threshold.

2 THERMODYNAMIC BACKGROUND

The system under consideration corresponds to a water-saturated porous plug (e.g. a cylindrical jacketed sample like use for permeability measurements). If equilibrium is perturbed by an increase of pore fluid pressure at one of its boundary, the porous body behaves as an open system exchanging energy, entropy, and matter with its

surrounding environment. One of the pillars of 'generalized' linear thermodynamics is the existence of a local equilibrium assumption, which is characterized by the use of the classic Gibbs-Duhem equation. Indeed Prigogine (1949) showed that the Gibbs-Duhem equation remains valid in the vicinity of equilibrium to the first-order of perturbation of the state variables. Neglecting deformation of the porous plug (e.g. poro-elastic effects) and assuming that the pore water is composed by a multicomponent (N species) electrolyte (N-1 ionic species plus the solvent), this yields:

$$du = T\,ds + \sum_{i=1}^{N} \tilde{\mu}_i\, dn_i, \tag{1}$$

where $\tilde{\mu}_i$ represents the electrochemical potential of the species i, n_i represents the concentration (in mol m^{-3}) of species i per unit volume of the porous plug, s and u represents the entropy and internal energy per unit volume of the porous plug, and T is the temperature (in K). For a 1:1 electrolyte saturating the pore space (e.g. NaCl or KCl), this yields:

$$T\frac{ds}{dt} = \frac{du}{dt} - \tilde{\mu}_{(+)}\frac{dn_{(+)}}{dt} - \tilde{\mu}_{(-)}\frac{dn_{(-)}}{dt} - \mu_w\frac{dn_w}{dt}, \tag{2}$$

where t is time (in s), d/dt represents the substantial time derivative, $n_{(\pm)}$ and n_w represent the concentrations of salt ions and water per unit volume of the porous plug, respectively, μ_w represents the total potential of water, and $\tilde{\mu}_{(\pm)} = \mu_{(\pm)} \pm e\psi$, represents the electrochemical potentials of the salt ions ($\mu_{(\pm)}$ represents the chemical potentials, e is the elementary charge, 1.19×10^{-19} C, the sign ± 1 depends on the sign of the charge carried by the ion, and ψ is the electric potential in V). The equations of continuity are:

$$\frac{du}{dt} = -\nabla \cdot \mathbf{w}, \tag{3}$$

$$\frac{dn_{(\pm)}}{dt} = -\nabla \cdot \mathbf{j}_{(\pm)}, \tag{4}$$

$$\frac{dn_w}{dt} = -\nabla \cdot \mathbf{j}_w, \tag{5}$$

where $\mathbf{w}$ represents the internal energy flux exchanged by the porous plug with its environment, and $\mathbf{j}_{(\pm)}$ and $\mathbf{j}_w$ represent the flux of ions and solvent (in mol m^2 s^{-1}), respectively. Eqs (2) to (5) yield,

$$\frac{ds}{dt} = -\frac{1}{T}\nabla \cdot \mathbf{w} + \frac{1}{T}\left(\tilde{\mu}_{(+)}\nabla \cdot \mathbf{j}_{(+)} + \tilde{\mu}_{(-)}\nabla \cdot \mathbf{j}_{(-)} + \mu_w \nabla \cdot \mathbf{j}_w\right), \tag{6}$$

$$\frac{ds}{dt} + \nabla \cdot \left[\frac{1}{T}\left(\mathbf{w} - \tilde{\mu}_{(+)}\mathbf{j}_{(+)} - \tilde{\mu}_{(-)}\mathbf{j}_{(-)} - \mu_w \mathbf{j}_w\right)\right] = \mathbf{w}\nabla\left(\frac{1}{T}\right) - \mathbf{j}_{(+)}\nabla\left(\frac{\tilde{\mu}_{(+)}}{T}\right) - \mathbf{j}_{(-)}\nabla\left(\frac{\tilde{\mu}_{(-)}}{T}\right) - \mathbf{j}_w\nabla\left(\frac{\mu_w}{T}\right), \tag{7}$$

$$\frac{ds}{dt} + \nabla \cdot \mathbf{j}_S = \Theta, \tag{8}$$

$$\mathbf{j}_S = \frac{1}{T}\left(\mathbf{w} - \tilde{\mu}_{(+)}\mathbf{j}_{(+)} - \tilde{\mu}_{(-)}\mathbf{j}_{(-)} - \mu_w \mathbf{j}_w\right), \tag{9}$$

$$\Theta = \mathbf{w}\nabla\left(\frac{1}{T}\right) - \mathbf{j}_{(+)}\nabla\left(\frac{\tilde{\mu}_{(+)}}{T}\right) - \mathbf{j}\nabla\left(\frac{\tilde{\mu}_{(-)}}{T}\right) - \mathbf{j}_w\nabla\left(\frac{\mu_w}{T}\right), \tag{10}$$

where $\mathbf{j}_S$ is the entropy flux vector (in Walt m^{-2}) and Θ represents the rate of inner entropy production (in Walt m^{-2}) in the porous plug (positive definite since entropy can only be created in the system during irreversible transformations). Eq. (8) represents a conservation equation for entropy. In isothermal conditions, the dissipation function of the system $D \equiv T\Theta \geq 0$ is given by:

$$D = -\mathbf{j}_{(+)}\nabla\tilde{\mu}_{(+)} - \mathbf{j}_{(-)}\nabla\tilde{\mu}_{(-)} - \mathbf{j}_w\nabla\mu_w. \tag{11}$$

Dissipation is zero at thermodynamic equilibrium. In linear thermodynamics, the choice of thermodynamic forces and fluxes is arbitrary to a certain extent as long as the product of any pair of conjugated flows and thermodynamic forces have the dimension of an entropy-production rate and the sum of all products leave the entropy production rate invariant. In addition needless to say that the material fluxes and scalar potentials are not uniquely defined and only the divergence of a flux and the gradient of a scalar potential have a physical meaning. This usually means that for experimental measurements, the choice of a reference state and a Lagrangian frame of reference represents crucial points.

Rather than using the ionic and solvent fluxes, geophysicists usually use the electrical current density $\mathbf{j}$ (in A m^{-2}) and Darcy filtration velocity $\mathbf{u}$ (in m s^{-1}) as independent fluxes in the hydroelectric problem (e.g. Ishido & Pritchett 1999). The Darcy velocity is here defined as the volume flow of solvent flowing per unit surface area and per unit time. In absence of macroscopic ionic concentration gradients, this yields $\mathbf{u} = \Omega_w \mathbf{j}_w$ and $\mathbf{j} = e(\mathbf{j}_{(+)} - \mathbf{j}_{(-)})$, where Ω_w is the molar volume of the solvent. The electrochemical potential of the ions and the chemical potential for the water phase are $\tilde{\mu}_{(\pm)} = (\pm)e\psi$ and $\mu_w = \Omega_w(p - \rho_f g z)$, respectively, where g is the gravity acceleration (in m s^{-2}) z is a vertical coordinate measured positively downward, and where I have neglected the concentration dependent component of the chemical potential of the pore water and therefore the osmotic pressure. Under these assumptions, the dissipation function is now given by,

$$D = -\mathbf{j}\nabla\psi - \mathbf{u}(\nabla p - \rho_f \mathbf{g}). \tag{12}$$

where $\mathbf{g} = g\mathbf{z}$, $\mathbf{z}$ being the unit vector along the vertical axis and directed downward. The two terms of eq. (12) correspond to the Joule and viscous dissipations of energy.

It is known, at least empirically, that irreversible flows are linear functions of the thermodynamic forces, as expressed by the phenomenological laws, which are introduced ad hoc to conform to experimental results. For example, Darcy's law expresses the observed fact that hydraulic flux is a linear function of the pore water pressure gradient. Ohm's law expresses that the electrical current is proportional to the electrical field. Also included in this type of linear relationships are the laws for such cross-phenomena as streaming potential (in which an electrical field is produced in response to the flow of pore water through a porous material) and electro-osmosis (in which a flow of pore water is produced in response to the application of an electrical field to a water-saturated porous material). In the vicinity of equilibrium, it is therefore safe to assume that all the fluxes are linearly dependent on all the forces operative in the system:

$$\mathbf{j} = -L_{11}\nabla\psi - L_{12}(\nabla p - \rho_f \mathbf{g}), \tag{13}$$

$$\mathbf{u} = -L_{21}\nabla\psi - L_{22}(\nabla p - \rho_f \mathbf{g}). \tag{14}$$

The condition $D \geq 0$ (as both T and Θ are positive) and the use of eqs (12) to (14) yields immediately $L_{12} = L_{21}$ (Onsager reciprocal law) (we note $\ell = L_{12} = L_{21}$ this coupling term, expressed in m^2 V^{-1} s^{-1}), $L_{ii} \geq 0$ (straight permeability coefficients definite positive), and $\ell^2 \leq L_{11}\,L_{22}$. Consequently, the open system is characterized by a set of 3 independent coefficients, $L_{11} = \sigma$ the electrical conductivity (in S m^{-1}) of the porous plug, $L_{22} = k/\eta_f$

the ratio between the intrinsic permeability k (in m^2) and the dynamic shear viscosity of the pore water η_f (in Pa s), and ℓ. The conservation equations for electrical charge is obtained combining eq. (4) with

$$\mathbf{j} = e\left(\mathbf{j}_{(+)} - \mathbf{j}_{(-)}\right),$$

$$\nabla \cdot \mathbf{j} = -d\rho/dt, \tag{15}$$

where $\rho = e(n_{(+)} - n_{(-)})$ represents the free charge density per unit volume of the porous rock. Eq. (5) and $\mathbf{u} = \Omega_w \mathbf{j}_w$ (and $n_w \Omega_w = \phi$ for a water saturated porous medium) yields:

$$\nabla \cdot (\rho_f \mathbf{u}) = -d(\rho_f \phi)/dt, \tag{16}$$

the conservation equation for the mass of the pore water. Now that the form of the macroscopic equations has been established, we discuss the relationship between the material properties entering these equations and the microstructural parameters of granular porous media.

3 MATERIAL PROPERTIES

Eqs (13) to (15) imply that the flow of pore water generates an electrical field called the streaming potential. The strength of this electrical field is determined by the streaming potential coupling coefficient C (in V Pa^{-1}):

$$C \equiv \left(\frac{\partial \Psi}{\partial p}\right)_{\mathbf{j}=\mathbf{0}} = -\frac{\ell}{\sigma}, \tag{17}$$

where $\Delta\Psi$ represents the electrical potential difference produced in response to a pore water pressure drop Δp imposed at the end faces of the jacketed cylindrical sample. In order to obtain the material properties of a granular porous medium with a random distribution of grains of the same size, different methods can be applied and combined. The volume averaging procedure of the local equations can be applied to a wide class of porous media (e.g. Pride 1994), and therefore to granular media as a specific case. For the electrical conductivity, a differential effective medium approach is a very efficient method to obtain the effective electrical conductivity as a function of the porosity (e.g. Sen *et al.* 1981). For granular porous media, the three independent coefficients entering into eqs (13) and (14) are related to two fundamental textural parameters characterizing the porous material F and Λ by

$$\sigma = \frac{\sigma_f}{F} \mathrm{H}(\xi), \tag{18}$$

$$\mathrm{H}(\xi) \equiv 1 - t_{(+)} + F\xi + \frac{1}{2}(t_{(+)} - \xi) \times \left(1 - \frac{\xi}{t_{(+)}} + \sqrt{\left(1 - \frac{1}{t_{(+)}}\xi\right)^2 + \frac{4F}{t_{(+)}}\xi}\right), \tag{19}$$

$$\ell \approx -\frac{\varepsilon_f \zeta}{\eta_f F}\left(1 - \frac{2\chi_d}{\Lambda}\right), \tag{20}$$

$$k = \frac{d^2}{\alpha F (F-1)^2}, \tag{21}$$

where eqs (18) and (19) result from the application of a differential effective medium approach (Revil *et al.* 1998), eq. (20) results from a volume-averaging approach (Pride 1994), and eq. (21) from a combination of both methods (Revil & Cathles 1999). In (18) and (19), σ_f represents the electrical conductivity of the pore water (in S m^{-1}), F is the electrical formation factor (dimensionless), $\xi = \sigma_S/\sigma_f$ is the ratio between surface to pore fluid electrical conductivity (dimensionless), σ_S represents the surface conductivity (in S m^{-1}), and $t_{(+)}$ is the Hittorf number of the cations in the electrolyte (dimensionless), which represents the fraction of electrical current transported by the cations in the pore water ($t_{(+)} = 0.38$ for NaCl and 0.51 for KCl). Surface conductivity corresponds to an electrical conduction mechanism located in the close vicinity of the pore water/mineral interface in the so-called electrical double layer coating the mineral water interface (e.g. Revil & Leroy 2001). In eq. (20), $\chi_d \equiv (\varepsilon_f k_b T/2e^2 I)^{1/2}$ is the Debye screening length (approximately half the thickness of the electrical double layer coating the pore water/mineral interface), k_b is the Boltzmann constant, I is the ionic strength in mol L^{-1} (∼salinity) of the pore water, ε_f is the dielectric constant of water $\sim(80 \times 8.84) \times 10^{-12}$ F m^{-1}, and ζ is the so-called ζ-potential, a key-property of the electrical double layer (e.g. Lorne *et al.* 1999; Pengra *et al.* 1999; Revil & Leroy 2001).

The correction term $(1 - 2\,\chi_d/\Lambda)$ (valid as long as $\chi_d \ll \Lambda/2$, Pride 1994) accounts for the finite thickness of the electrical double layer by comparison with the characteristic length Λ controlling transport in the connected pore space (see Kostek *et al.* 1992 and Wildenschild *et al.* 2000 for a description of the characteristic length Λ, which corresponds to an effective pore throat radius controlling the transport properties through the connected porosity). This length scale is not a geometrical parameter and therefore cannot be measured directly. However, it is a very convenient parameter to use in the purpose to unify transport properties of porous materials (Kostek *et al.* 1992). In (21), d is the mean diameter of the grains and α is a numerical constant depending on the pore space topology (Section 4). For granular materials composed by uniform grains of diameter d, the formation factor F and the Λ-parameter are given by (e.g. Revil & Cathles 1999):

$$F = \phi^{-m}, \tag{22}$$

$$\Lambda = \frac{d}{2m(F-1)}, \tag{23}$$

where m represents a grain shape parameter related to the shape distribution of the grains (Sen *et al.* 1981). Eqs (22) and (23) have actually the same status as they can both be derived using a differential effective medium approach applied to the determination of the electrical conductivity of a representative elementary volume of a granular porous medium (Revil & Cathles 1999). Eq. (22) should not be mislead with the Archie's law, which, in the original paper by Archie (1942), applies only to the porosity/formation factor correlation of a set of samples coming from the same formation reservoir. In the high porosity limit ($\phi \to 1$) corresponding to a dilute suspensions of spheres, $m = 1.5$ (e.g. Sen *et al.* 1981), (22) and (23) tend to

$$F = \phi^{-3/2} \to 1 + \frac{3}{2}\left(\frac{1-\phi}{\phi}\right), \tag{24}$$

$$\Lambda \to \frac{2\phi\, d}{9(1-\phi)}. \tag{25}$$

Eq. (24) represents the well-known Hashin-Shtrikman lower bound and (25) is similar to eq. (24c) of Kostek *et al.* (1992). The Hashin-Shtrikman lower bound is known to be fairly accurate in the limit of dilute suspensions of spherical particles whatever its geometry. At high fractional connected porosity ($\phi \gg \phi_p$, say $\phi > 0.40$) F can be replaced by its asymptotic limit and (21) reaches a well-known asymptotic limit:

$$k \approx \left(\frac{8}{27\alpha}\right)\frac{d^2\phi^3}{(1-\phi)^2}, \tag{26}$$

which corresponds to the Kozeny-Carman relationship with $\alpha \approx 53$ (e.g. Carman 1937). In the high porosity limit, the Kozeny-Carman relationship is a fairly good indicator of the permeability. However, the Kozeny-Carman relationship fails to predict accurately the permeability at porosity below 0.30 (Revil & Cathles 1999, their Fig. 5).

One of the purposes of this note is to improve the predictive capability of (18) to (21) at porosity below 0.30. This can be done by introducing a percolation porosity in the electrical formation factor/porosity relationship and therefore in the transport properties described by eqs (18) to (21):

$$F = (\phi - \phi_p)^{-m}, \tag{27}$$

where ϕ_p represents the percolation porosity. Eq. (27) can be seen as an attempt to force a percolation threshold into an equation obtained from the use of differential effective medium theory, which excludes, by construction, any percolation threshold. The percolation porosity corresponds to the minimum value of the connected porosity at which connected paths through the representative elementary volume exist. The value of ϕ_p depends on the porosity reduction mechanism, e.g. mineral precipitation, pressure solution. For example, if the diameter of the grains growths uniformly during the porosity reduction process, the percolation porosity is expected to be in the range ~0.02–0.05 (for an sc-packing of spheres of same diameter, $\phi_p \approx 0.035$, Roberts & Schwartz (1985); Schwartz & Kimminau (1987). Near percolation of course, any type of modeling based on the notion of elementary representative volume is in principle not valid as heterogeneities have the same size as the volume investigated. Using percolation concepts, Guéguen & Palciauskas (1992) obtained a formation factor/porosity relationship $F \sim (\phi - \phi_p)^{-2}\, \phi^{-1}$ quite similar to eq. (27). I show below that the introduction of a percolation threshold in eqs (18) to (21) improves clearly the predictive capabilities of these equations down to very low porosities.

4 ELECTRICAL CONDUCTIVITY

I test here the validity of the electrical conductivity/formation factor relationship using the data obtained by Lorne *et al.* (1999, their Fig. 5) (crushed Fontainebleau sandstone with a mean grain diameter ~80 μm). Eqs (18) and (19) provide an excellent fit of the experimental data from Lorne *et al.* (1999) in the entire salinity range above the iso-conductivity point characterized by the condition $\sigma = \sigma_f$ (see Fig. 1a). The specific surface conductivity Σ_S (in S) represents the excess electrical conductivity associated with the excess of ions located in the electrical double layer (Revil & Leroy 2001). The specific surface conductivity is related to σ_S and the mean grain diameter d of the porous aggregate by $\sigma_S = 4\,\Sigma_S/d$ (e.g. Revil & Leroy 2001). Using $d = 80$ μm and the surface conductivity determined in Fig. 1(a) using eqs (18) and (19), I obtain $\Sigma_S = (2.1 \pm 0.4) \times 10^{-9}$ S. This value is in the same range with that determined independently from the double layer model of Revil & Leroy (2001), which is $(1.6 \pm 0.3) \times 10^{-9}$ S at pH 7.

For granular porous materials, formation factor versus porosity data are shown in Fig. 1(b). For an assemblage of perfect spheres, the differential effective medium theory predicts a porosity/formation factor relationship, eq. (22), with $m = 1.5$ (Sen *et al.* 1981). In Fig. 1(b), we compare three estimates to evaluate the formation factor/porosity relationship. They are eq. (22) with $m = 1.5$, the Hashin-Shtrikman lower bound, eq. (24), and the modified porosity/formation factor relationship with a percolation porosity, eq. (27) with $m = 1.5$. The inclusion of a percolation threshold in the formation factor/porosity relationship improves clearly the ability of the porosity/formation factor to predict the F versus ϕ trend at porosity below 0.25. The data reported in Fig. 1(b) yields a percolation porosity ~0.025 in agreement with that determined for porous rocks by Roberts & Schwartz (1985) and Schwartz & Kimminau (1987) with unimodal and very narrow grain size distributions.

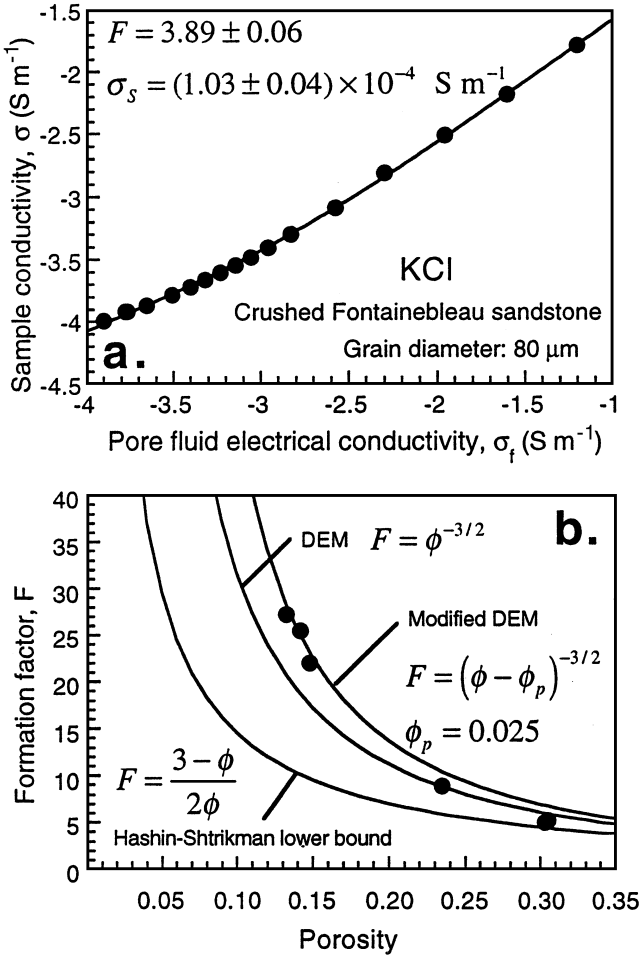

Figure 1. (a) Electrical conductivity of a crushed Fontainebleau sandstone versus pore water conductivity (data from Lorne *et al.* 1999, grain size 80 μm, pH 5.7, electrolyte is KCl and therefore $t_{(+)} = 0.51$). The electrical formation factor and the surface conductivity are determined from a best fit of the electrical conductivity model described in the main text and materialized by the plain line. (b) Electrical formation factor versus porosity. Comparison between the predictions of the modified differential effective medium theory with a percolation threshold, the classical effective medium theory (DEM), and the Hashin-Shtrikman lower bound (the filled black circles corresponds to the experimental data from Johnson *et al.* 1982).

5 PERMEABILITY

As explained in Section 3, there is a relationship between hydraulic and electrical transport properties. If we note σ_S the equivalent conductivity of a grain coated with the electrical double layer, a simple arithmetic average of the electrical conductivity of the porous medium yields $\sigma = \phi\,\sigma_f + (1 - \phi)\,\sigma_S$. In real porous materials, the porosity should be replaced by the inverse of the electrical formation factor, which represents by definition the efficient surface area for the electromigration of the ions through the connected pore space. This yields:

$$\sigma = \frac{1}{F}[\sigma_f + (1 - F)\sigma_S]. \tag{28}$$

According to volume averaging arguments, the electrical conductivity of a porous material σ in the high salinity limit is also given by (e.g. Pride 1994),

$$\sigma = \frac{1}{F}\left[\sigma_f + \frac{2}{\Lambda}\Sigma_S + \cdots\right], \tag{29}$$

where the specific surface conductivity Σ_S is related to σ_S by $\sigma_S = 2\,\Sigma_S/R$ where $R = 2\,d$ is the radius of the grains. Comparison between eqs (28) and (29) yields $\Lambda = d/[2(F-1)]$, which result is slightly different from eq. (23). A relationship between the permeability and the length scale Λ is given by $k = \Lambda^2/a\,F$ with usually $4 \leq a \leq 8$ (Pride 1994). Incorporating $\Lambda = d/[2(F-1)]$ in this relationship yields eq. (21) with $\alpha = 4\,a$.

In Figs 2(a) and (b), our modified permeability model is tested against the data reported by Spangenberg *et al.* (1998) for salt rocks and Chilindar (1964) for natural sandstones. In the first case, we check the relationship between k and F using $\alpha = 8$. We obtain an excellent agreement between eq. (21) and the experimental data reported by Spangenberg *et al.* (1998) over six orders of magnitude. In Fig. 2(b), permeability versus porosity data show the necessity to incorporate a percolation threshold in the equations. For these types of sandstone, this yields a percolation porosity ~0.025 like in Section 3.

6 STREAMING POTENTIAL COUPLING COEFFICIENT

Introduction of a percolation threshold in the electrokinetic coupling coefficient C is performed taking eq. (17) and using (18) to (20),

$$C = \frac{C_{\rm HS}}{\mathrm{H}(\xi)}\left[1 - 4m(F-1)\frac{\chi_d}{d}\right], \tag{30}$$

$$C_{\rm HS} \equiv \frac{\varepsilon_f \zeta}{\eta_f \sigma_f}, \tag{31}$$

where $C_{\rm HS}$ is the streaming potential coupling coefficient corresponding to the Helmholtz-Smoluchowski (HS) formula. The HS formula is widely used in an important number of publications to interpret electrokinetic laboratory experiments or field data. It predicts that the streaming potential coupling coefficient does not depend on the microstructure of the porous medium. Actually, experimental data reported in the literature showed that the streaming potential coupling coefficient depends quite strongly on the microgeometry of the porous medium at porosity below 0.30 (e.g. Bull & Gortner 1932). Actually the HS formula is valid only at very high salinity and/or high porosity where the two conditions $\mathrm{H}(\xi \ll 1) = 1 + \mathrm{O}(\xi) + \cdots$ and $\chi_d \ll d/[4(F-1)]$ are simultaneously satisfied. According to eqs (30) and (31), the streaming potential coefficient depends generally on the porosity. The normalized streaming potential coefficient $C/C_{\rm HS}$ is shown as a function of the porosity in Fig. 3(a). The model predicts that the ratio $C/C_{\rm HS}$ increases strongly with the porosity, especially at low salinity. This prediction is very well confirmed by the experimental data reported by Jouniaux & Pozzi (1995) (Fig. 3b). The surface conductivity determined from eqs (30) and (31) and the data by Jouniaux & Pozzi (1995) is $\sigma_S = 0.84 \times 10^{-4}\ \mathrm{S\,m^{-1}}$, which is in good agreement with that determined independently from electrical conductivity data in Fig. 1(a) ($\sigma_S = 1.03 \times 10^{-4}\ \mathrm{S\,m^{-1}}$). In addition the data of Fig. 3(b) show a good agreement with a model including a percolation threshold at low porosity. For the Fontainebleau sandstone, this yields a percolation porosity ~0.035 ± 0.10, quite similar to the value reported in Sections 3 and 4 (0.025).

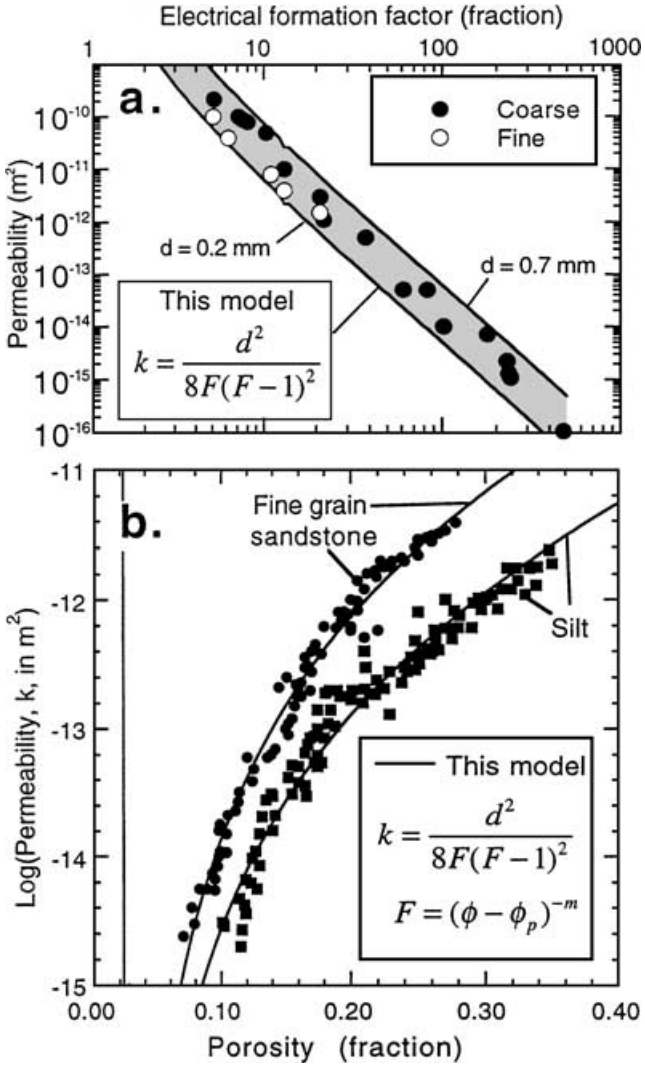

Figure 2. (a) Permeability versus electrical formation factor (data from Spangenberg *et al.* 1998, their Fig. 6, and corresponding to salt rocks). The initial mean grain diameter of the samples is in the range 0.5–2 mm for the coarse-grained samples and 0.1–0.5 mm for the fine-grained samples. (b) Comparison between the model and the data from Chilindar (1964, Fig. 2, p. 73) (fine and silty-grained natural sandstone naturally compacted). Parameter used: $m = 1.5$, $\phi_p = 0.025$ and the best fit of the model with the experimental data yields $d = 116\ \mu$m for the fine-grained sandstone (filled circles) and 46 μm for the silt (filled squares).

7 CONCLUDING STATEMENTS

In this paper, I show (1) how the hydroelectric equations result from the Gibbs-Duhem equation and (2) that the three materials properties (electrical conductivity, permeability, and electrokinetic coupling coefficient) entering the hydroelectric equations exhibit a similar percolation porosity. For sandstones and granular materials, the percolation porosity is in the range 0.02–0.04, which is quite small. For other types of porous rocks like vesicular basalts, it is expected that this percolation porosity could be much higher than the previous value owing to their different texture.

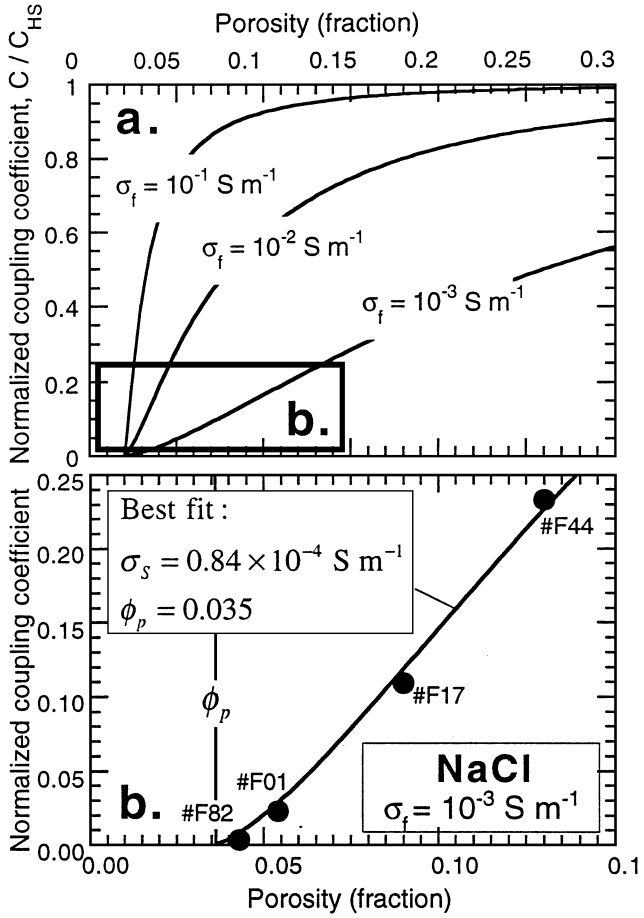

Figure 3. (a) Normalized streaming potential coupling coefficient versus porosity. Parameters used: $m = 1.5$, $\phi_p = 0.02$, and $\sigma_S = 1 \times 10^{-4}$ S m^{-1}. (b) Influence of the porosity upon C. Comparison between the data reported by Jouniaux & Pozzi (1995, Table 1 samples #F82, F17, F01 and F44) and the model described in the main text. Parameters used: $\sigma_f = 1 \times 10^{-3}$ S m^{-1} (NaCl, measured), $\zeta = -40$ mV (from Lorne *et al.* 1999, measured their Fig. 20), $\varepsilon_f = 7.1 \times 10^{-10}$ F m^{-1}, and $\eta_f = 1.0 \times 10^{-3}$ Pa s. The porosity of samples F17 and F01 is determined from the permeability/porosity trend typical of the Fontainebleau sandstone and the permeability data reported for these samples in Jouniaux & Pozzi (1995, Table 1) (uncertainty better than 10 per cent in relative value). A non-linear fit of the data is performed using the model developed in the main text. The values of surface conductivity and percolation porosity are reported on the graph.

ACKNOWLEDGMENTS

I am grateful to Frédéric Perrier for fruitful discussions and the two referees for their useful comments. I thank the Ministère de l'Education Nationale de la Recherche et de la Technologie (MENRT) in France (ACI Jeunes and ACI 'Eau et Environnement') and the French National Research Council (CNRS). B. Dupré, M. Cara, P. Choukroune, and B. Hamelin are especially thanked for encouraging supports during the last three years.

REFERENCES

Archie, G.E., 1942. The electrical resistivity as an aid in determining some reservoir characteristics, *J. Pet. Tech.,* **5,** 1.

Birch, F.S., 1998. Imaging the water table by filtering self-potential profiles, *Ground Water,* **36,** 779–782.

Bull, H.B. & Gortner R.A., 1932. Electrokinetic potentials, X. The effect of particle size on the potential, *J. Phys. Chem.,* **36,** 111–119.

Carman, P.C., 1937. Fluid flow through a granular bed, *Trans. Inst. Chem. Eng. London,* **15,** 150–156.

Chilindar, G.V., 1964. Relationship between porosity, permeability and grain size distribution of sands and sandstones, in *Deltaic and Shallow Marine Deposits,* Vol. I, pp. 71–75, ed. Van Straaten, L.M.J.U., Elsevier, New York.

Guéguen, Y. & Palciauskas, V., 1992. Introduction à la Physique des Roches, Hermann, Paris, p. 299.

Ishido, T. & Pritchett, J.W., 1999. Numerical simulation of electrokinetic potentials associated with subsurface fluid flow, *J. geophys. Res.,* **104,** 15 247–15 259.

Johnson, D.L., Plona, T.J., Scala, C., Pasierb, F. & Kojima, H., 1982. Tortuosity and acoustic slow waves, *Phys. Rev. Lett.,* **49,** 1840–1844.

Jouniaux, L. & Pozzi, J.-P., 1995. Streaming potential and permeability of saturated sandstones under triaxial stress: consequences for electrotelluric anomalies prior to earthquake, *J. geophys. Res.,* **100,** 10 197–10 209.

Kostek, S., Schwartz, L.M. & Johnson, D.L., 1992. Fluid permeability in porous media: comparison of electrical estimates with hydrodynamical calculations, *Phys. Rev. B,* **45,** 186–195.

Lorne, B., Perrier, F. & Avouac, J.-P., 1999. Streaming potential measurements. 1. Properties of the electrical double layer from crushed rock samples, *J. geophys. Res.,* **104,** 17 857–17 877.

Pengra, D.B., Li, S.X. & Wong, P., 1999. Determination of rock properties by low-frequency AC electrokinetics, *J. geophys. Res.,* **104,** 29 485–29 508.

Pride, S.R., 1994. Governing equations for the coupled electromagnetics and acoustics of porous media, *Phys. Rev. B,* **50,** 15 678–15 696.

Prigogine, I., 1949. Le domaine de validité de la thermodynamique des phénomènes irréversibles, *Physica,* **15,** 272–284.

Revil, A. & Cathles, L.M., 1999. Permeability of shaly sands, *Water Resour. Res.,* **35,** 651–662.

Revil, A. & Leroy, P., 2001. Hydroelectric coupling in a clayey material, *Geophys. Res. Lett.,* **28,** 1643–1646.

Revil, A., Cathles, L.M., Losh, S. & Nunn, J.A., 1998. Electrical conductivity in shaly sands with geophysical applications, *J. geophys. Res.,* **103,** 23 925–23 936.

Revil, A., Naudet, V., Nouzaret, J. & Pessel, M., Principles of electrography applied to self-potential electrokinetic sources and hydrogeological applications, *Water Resources Research*.

Revil, A., Hermitte, D., Voltz, M., Moussa, R., Lacas, J.-G., Bourrié, G. & Trolard, F., 2002. Self-potential signals associated with variations of the hydraulic head during an infiltration experiment, *Geophys. Res. Lett.,* **10,** 1029/2001GL014294.

Roberts, J.N. & Schwartz, L.M., 1985. Grain consolidation and electrical conductivity in porous media, *Phys. Rev.,* **31,** 5990–5997.

Schwartz, L.M. & Kimminau, S., 1987. Analysis of electrical conduction in the grain consolidation model, *Geophysics,* **52,** 1402–1411.

Sen, P.N., Scala, C. & Cohen, M.H., 1981. Self-similar model for sedimentary rocks with application to the dielectric constant of fused glass beads, *Geophysics,* **46,** 781–795.

Spangenberg, E., Spangenberg, U. & Heindorf, C., 1998. An experimental study of transport properties of porous rock salt, *Phys. Chem. Earth,* **23,** 367–371.

Trique, M., Richon, P., Perrier, F., Avouac, J.P. & Sabroux, J.C., 1999. Radon emanation and electric potential variations associated with transient deformation near reservoir lakes, *Nature,* **399,** 137–141.

Wildenschild, D., Roberts, J.J. & Carlberg, E.D., 2000. On the relationship between microstructure and electrical and hydraulic properties of sand-clay mixtures, *Geophys. Res. Lett.,* **27,** 3085–3088.